Observation of amplitude and phase in ridge and photonic crystal waveguides operating at 1.55 μm by use of heterodyne scanning near-field optical microscopy

P. Tortora

Institute of Microtechnology, University of Neuchâtel, Rue A.-L. Breguet 2, 2000 Neuchâtel, Switzerland

M. Abashin

Department of Electrical and Computer Engineering, University of California, San Diego, 9500 Gilman Drive, La Jolla, California 92093-0407

I. Märki, W. Nakagawa, L. Vaccaro, M. Salt, and H. P. Herzig

Institute of Microtechnology, University of Neuchâtel, Rue A.-L. Breguet 2, 2000 Neuchâtel, Switzerland

U. Levy and Y. Fainman

Department of Electrical and Computer Engineering, University of California, San Diego, 9500 Gilman Drive, La Jolla, California 92093-0407

Received April 26, 2005; revised manuscript received July 7, 2005; accepted July 9, 2005

We apply heterodyne scanning near-field optical microscopy (SNOM) to observe with subwavelength resolution the amplitude and phase of optical fields propagating in several microfabricated waveguide devices operating around the 1.55 μm wavelength. Good agreement between the SNOM measurements and predicted optical mode propagation characteristics in standard ridge waveguides demonstrates the validity of the method. *In situ* observation of the subwavelength-scale distribution and propagation of optical fields in straight and 90° bend photonic crystal waveguides facilitates a more detailed understanding of the optical performance characteristics of these devices and illustrates the usefulness of the technique for investigating nanostructured photonic devices. © 2005 Optical Society of America

OCIS codes: 040.2840, 120.5050, 180.5810, 230.7370.

Photonic nanostructures, and in particular photonic crystals (PCs), provide a number of possibilities for developing novel devices based on near-field optical phenomena, as well as for monolithic integration of large-scale photonic systems.[1–3] However, as many of these devices depend on the subwavelength-scale localization of optical fields, traditional far-field characterization techniques are incapable of fully capturing the propagation characteristics of light in such structures. Scanning near-field optical microscopy[4,5] (SNOM) provides the ability to observe directly the optical fields propagating in a photonic structure with subwavelength resolution and has been applied to investigate PC resonators and various other devices.[6,7] In heterodyne SNOM, light collected by the scanning probe is combined with a frequency-shifted reference beam to permit simultaneous measurement of the local amplitude and phase of the probed field.[8–10] This technique has been used to characterize several devices, including periodically structured waveguides[11] and structured optical fibers,[12] demonstrating the usefulness of SNOM for the detailed characterization of optical field propagation inside microstructured waveguides. In this Letter, we apply this technique to investigate microfabricated ridge and PC waveguides and demonstrate the measurement of the phase and amplitude of the propagating fields in silicon-based photonic devices at the 1.55 μm wavelength.[13] The obtained results are in good agreement with predicted values, illustrating the viability of the technique as a method for investigating the complex amplitude of optical fields as they propagate inside the waveguides, and could have a significant effect on the understanding and development of nanostructured optical devices.

In the present setup, the source is a semiconductor cw laser operating in a wavelength band around 1.55 μm. The cantilevered tapered fiber probe has an aperture of 200 nm and is scanned in tapping mode. This scanning technique reduces lateral interaction forces and is particularly advantageous for the investigation of silicon membranes or other fragile samples having abrupt topographical changes.

First, we characterize a standard ridge waveguide. This device is fabricated using a silicon-on-insulator wafer with an approximately 290 nm thick silicon guiding layer on a 1 μm thick oxide layer. The waveguide structure consists of 10 μm wide input and output sections, a 0.5 μm wide section at the center, and linearly tapered sections in between to connect them. The oxide separation layer under the thin central section of the waveguide is undercut, resulting in an air-bridge structure.

The detected topography, amplitude, and phase for 1.55 μm light with polarization orthogonal to the substrate plane propagating in a 25 μm long seg-

0146-9592/05/212885-3/$15.00

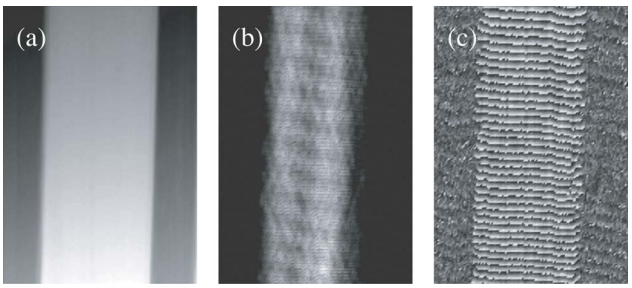

Fig. 1. SNOM images of a 25 μm long segment of the wide (10 μm width) section of the tapered ridge waveguide showing (a) topography, (b) amplitude, and (c) phase measurements.

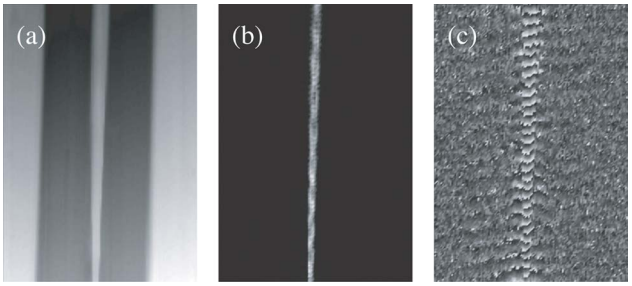

Fig. 2. SNOM images of a 25 μm long segment of the tapered and air bridge (0.5 μm width) sections of the ridge waveguide device showing (a) topography, (b) amplitude, (c) and phase measurements.

ment of the wide section of the waveguide are shown in Fig. 1. Comparison of the amplitude map [Fig. 1(b)] with the topography [Fig. 1(a)] clearly shows good confinement of the light in the waveguide region. The phase map [Fig. 1(c)] confirms the same observation and shows a planar phase front, indicating that most of the light propagates in the fundamental mode. The Fourier transform of the measured complex amplitude along the propagation direction shows the strongest frequency component—corresponding to the dominant propagating mode—to have an effective wavelength of approximately 0.57 μm, very close to the predicted value of 0.61 μm for the fundamental TM-like mode.

In Fig. 2, we report measurements performed on the narrow air-bridge section of the waveguide. The topography [Fig. 2(a)] shows that part of the ridge and the initial part of the output taper are included in the scan. The amplitude [Fig. 2(b)] and phase [Fig. 2(c)] images show that the light is once again well confined in the waveguide. The spacing of the phase fronts in the taper section [top portion of Fig. 2(c)] can be seen to be different from in the air-bridge section. The periodic oscillations in the amplitude of Fig. 2(b) are due to a Fabry–Perot standing wave pattern in the waveguide. The Fourier transform of the complex amplitude data for the narrow waveguide section (excluding the taper) shows that the effective wavelength of the propagating mode is 0.77 μm. Numerical simulation of the waveguide design yields 0.76 μm for the effective wavelength. The excellent agreement between the predicted and measured optical propagation characteristics demonstrates the capability of this heterodyne SNOM to characterize photonic devices operating in the 1.55 μm wavelength regime.

Next, we apply the heterodyne SNOM to the characterization of PC waveguides. The PC lattice consists of a square array of microfabricated cylindrical holes in a thin silicon membrane surrounded by air. The design parameters of the PC structure are lattice constant $a=496$ nm, hole radius $r=190$ nm, and slab thickness $t=290$ nm. These values are chosen to give rise to a TE-like (in-plane polarization) photonic bandgap for wavelengths around 1.5 μm. The waveguide is formed by eliminating a single row of holes such that the propagating modes are confined within the defect. Two different PC devices are studied, a straight waveguide and a 90° bend. To facilitate injection of light into the waveguide, tapered ridge waveguides identical to the previous example are used.

The straight (PC) waveguide device, shown in Fig. 3(a), has a length of 30 μm. In previous work using this device, high transmission efficiency was measured in the wavelength range of 1530 to 1590 nm, efficient coupling from the ridge waveguide to the PC waveguide was observed, and the propagation loss in the PC waveguide was estimated to be of the order of 25 dB/mm.[14,15] Using the heterodyne SNOM, we observe over 14 μm the amplitude and phase of light with wavelength 1560 nm propagating through the structure, as shown in Figs. 3(b) and 3(c), respectively. In the amplitude image we observe a confined propagating mode along the defect guide. A weak signal can be detected in the PC region around the defect guide indicating that a small amount of light is leaking into the PC. The phase image clearly shows a distinct phase front corresponding to the propagating mode inside the defect guide. The horizontal wavefront profile indicates that most of the light is propagating in the first defect mode having an even transverse symmetry, this being expected according to the modal analysis discussion in Ref. 15.

The last example is a PC waveguide with a 90° bend, as shown in Fig. 4(a). The measured amplitude and phase of light with a wavelength of 1550 nm

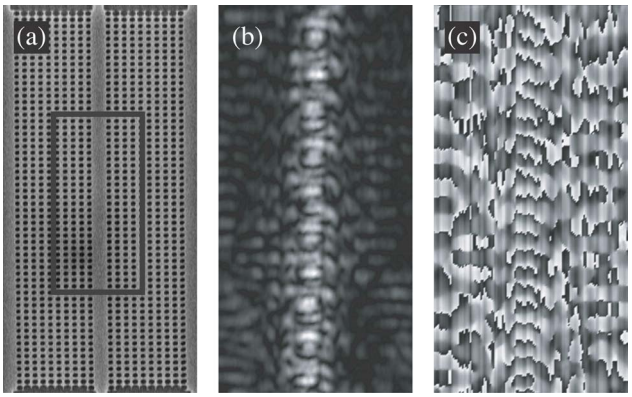

Fig. 3. Straight PC waveguide: (a) top-view scanning electron microscope image of the device (the square outline indicates the approximate SNOM measurement area); (b) SNOM amplitude measurement of the propagating mode in the waveguide over an area of 7 μm $\times$ 14 μm; (c) SNOM phase measurement.

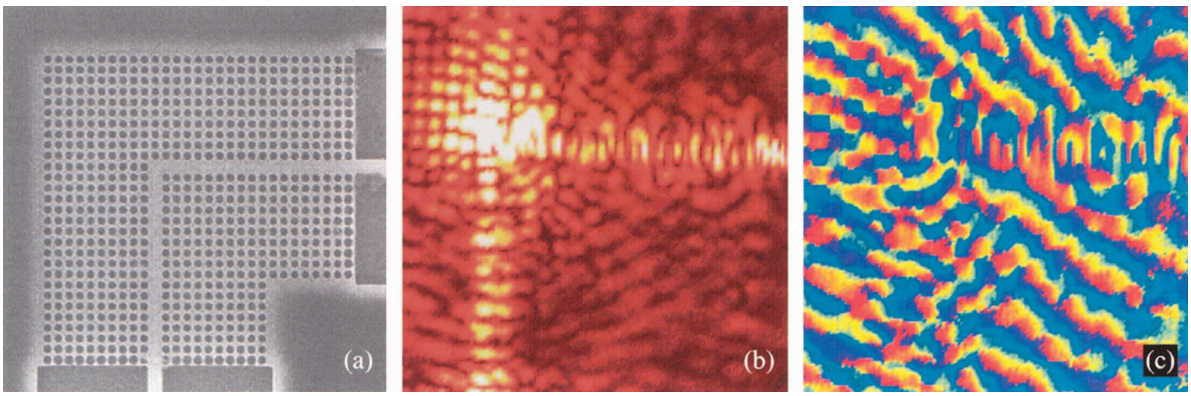

Fig. 4. Images of the PC waveguide 90° bend structure: (a) SEM, (b) SNOM amplitude, (c) SNOM phase.

propagating in the waveguide are shown in Figs. 4(b) and 4(c), respectively. Good confinement of the light in the waveguide channel is observed in both straight waveguide segments. In addition, in the input arm of the device (propagating up from the bottom of the figure), the dominant mode corresponds to the first defect mode having an even transverse symmetry, while the more complex variations in the transverse field profile in the output arm suggest a superposition of multiple modes having even and odd transverse symmetry. Simulations have shown that coupling to higher-order modes in the PC corner occurs due to the broken symmetry at the corner.[15] Finally, in the region of the waveguide bend, significant penetration of the light into the PC lattice is observed. A significantly higher amplitude signal is detected by the SNOM in this region because of two mechanisms: first, the corner region acts as a resonant cavity, resulting in a significantly higher field amplitude inside; and second there is significantly greater leakage or scattering of light from the vicinity of the corner, as compared with the straight waveguides. These preliminary measurements on the PC waveguides demonstrate the capabilities of the technique; however, a more comprehensive investigation of the optical propagation characteristics in such structures requires further study.

We have demonstrated the direct observation of the amplitude and phase of an optical field propagating in ridge and PC silicon on insulator–based waveguides for wavelengths around 1.55 μm by use of heterodyne SNOM. These results are consistent with predicted values from previous numerical or far-field experimental studies. These results also show the usefulness of the heterodyne SNOM as an investigative and diagnostic tool in the study of optical propagation in nanostructures, in particular in cases where subwavelength-scale and near-field effects are important. In the future, this technique can be applied to a wide range of PC and other nanostructure-based photonic devices, facilitating the improved understanding of nanoscale optical phenomena and the design and optimization of nanostructured photonic devices and systems.

The authors acknowledge assistance from R. Rokitski and K. Tetz (Department of Electrical and Computer Engineering, University of California, San Diego) in adapting the SNOM system for the purposes of these measurements and thank F. Schädelin, S. Gautsch, U. Staufer, and N. F. de Rooij (Institute of Microtechnology, University of Neuchâtel) for the fabrication of the waveguide and photonic crystal samples. The authors also acknowledge the support of the NSF, DARPA, and the AFOSR, as well as the Swiss National Science Foundation. P. Tortora's e-mail address is piero.tortora@unine.ch.

References

1. S. G. Johnson, A. Mekis, S. Fan, and J. D. Joannopoulos, Comput. Sci. Eng. **3**, 38 (2001).
2. S. Noda, M. Imada, M. Okano, S. Ogawa, M. Mochizuki, and A. Chutinan, IEEE J. Quantum Electron. **38**, 726 (2002).
3. M. Notomi, A. Shinya, S. Mitsugi, E. Kuramochi, and H.-Y. Ryu, Opt. Express **12**, 1551 (2004).
4. U. Dürig, D. W. Pohl, and F. Rohner, J. Appl. Phys. **59**, 3318 (1986).
5. H. Heinzelmann and D. W. Pohl, Appl. Phys. A **59**, 89 (1994).
6. K. Okamoto, M. Loncar, T. Yoshie, A. Scherer, Y. Qiu, and P. Gogna, Appl. Phys. Lett. **82**, 1676 (2003).
7. P. Kramper, M. Kafesaki, C. M. Soukoulis, A. Birner, F. Muller, U. Gosele, R. B. Wehrspohn, J. Mlynek, and V. Sandoghdar, Opt. Lett. **29**, 174 (2004).
8. M. L. M. Balistreri, J. P. Korterik, L. Kuipers, and N. F. van Hulst, Phys. Rev. Lett. **85**, 294 (2000).
9. A. Nesci, R. Dändliker, and H. P. Herzig, Opt. Lett. **26**, 208 (2001).
10. S. I. Bozhevolnyi and B. Vohnsen, Opt. Commun. **212**, 217 (2002).
11. E. Flück, M. Hammer, A. M. Otter, J. P. Korterik, L. Kuipers, and N. F. van Hulst, J. Lightwave Technol. **21**, 1384 (2003).
12. J. C. Gates, C. W. J. Hillman, J. C. Baggett, K. Furusawa, T. M. Monro, and W. S. Brocklesby, Opt. Express **12**, 847 (2004).
13. A. Nesci and Y. Fainman, in Proc. SPIE **5181**, 62 (2003).
14. I. Märki, M. Salt, and H. P. Herzig, J. Appl. Phys. **96**, 7 (2004).
15. I. Märki, M. Salt, R. Stanley, U. Staufer, and H. P. Herzig, J. Appl. Phys. **96**, 6966 (2004).